The Global Distribution and Drivers of Grazing Dynamics Estimated from Inverse Modelling

Tyler Rohr[1]

[1]Institute for Marine and Antarctic Science, University of Tasmania, Hobart, Tasmania, 7000, Australia

December 8, 2022

Abstract

We examine how zooplankton influence phytoplankton bloom phenology from the top-down, then use inverse modelling to infer the distribution and drivers of mean community zooplankton grazing dynamics based on the skill with which different simulated grazing formulations are able to recreate the observed seasonal cycle in phytoplankton biomass. We find that oligotrophic (eutrophic) biomes require more (less) efficient grazing dynamics, characteristic of micro- (meso-) zooplankton, leading to a strong relationship between the observed mean annual phytoplankton concentration in a region and the optimal grazing parameterization required to simulate it's observed phenology. Across the globe, we found that a type III functional response consistently exhibits more skill than a type II response, suggesting the mean dynamics of a coarse model grid-cell should offer stability and prey refuge at low biomass concentrations. These new observationally-based global distributions will be invaluable to help constrain, validate and develop next generation of biogeochemical models.

The Global Distribution and Drivers of Grazing Dynamics Estimated from Inverse Modelling

Tyler Rohr[1,2], Anthony Richardson[3,4], Andrew Lenton[5], Matt Chamberlain[5], Elizabeth Shadwick[2,5]

[2]Intsitute for Marine and Antarctic Science, University of Tasmania, Hobart, Tasmania, 7000, Australia

[2]Australian Antarctic Partnership Program, Hobart, Tasmania, 7000, Australia

[3]School of Mathematics and Physics, The University of Queensland, St Lucia, Queensland, Australia

[4]Commonwealth Scientific and Industrial Research Organisation (CSIRO) Oceans and Atmosphere,

BioSciences Precinct (QBP), St Lucia, Queensland, 4067, Australia

[5]Commonwealth Scientific and Industrial Research Organisation (CSIRO) Oceans and Atmosphere,

Hobart, Tasmania, 7000 Australia

Key Points:

- Oligotrophic (eutrophic) biomes exhibit more (less) efficient mean community grazing dynamics, characteristic of micro- (meso-) zooplankton.
- There is a strong relationship between mean phytoplankton biomass and the grazing dynamics required to simulate its observed seasonal cycle.
- A type III response does a consistently better job of recreating observed phytoplankton phenology compared to a type II response.

Corresponding author: Tyler Rohr, `tyler.rohr@csiro.au`

Abstract

We examine how zooplankton influence phytoplankton bloom phenology from the top-down, then use inverse modelling to infer the distribution and drivers of mean community zooplankton grazing dynamics based on the skill with which different simulated grazing formulations are able to recreate the observed seasonal cycle in phytoplankton biomass. We find that oligotrophic (eutrophic) biomes require more (less) efficient grazing dynamics, characteristic of micro- (meso-) zooplankton, leading to a strong relationship between the observed mean annual phytoplankton concentration in a region and the optimal grazing parameterization required to simulate it's observed phenology. Across the globe, we found that a type III functional response consistently exhibits more skill than a type II response, suggesting the mean dynamics of a coarse model grid-cell should offer stability and prey refuge at low biomass concentrations. These new observationally-based global distributions will be invaluable to help constrain, validate and develop next generation of biogeochemical models.

Plain Language Summary

To improve our predictions of the ocean's ability to feed a growing human population and buffer a changing climate we must improve our understanding of what happens to carbon once it is absorbed into the ocean. One of the largest gaps in marine carbon cycling is the role of zooplankton grazing. The rate at which zooplankton graze (or consume) phytoplankton modifies the size and seasonal evolution of both populations and in turn their associated rates of net primary production (the base of the food chain), secondary production (an indicator of fisheries catch) and export production (the biological sequestration of carbon). However, regional differences in in-situ grazing dynamics, which cannot be directly measured outside of a laboratory, remain poorly constrained by observations and thus difficult to model. Here, we run many model simulations, each of which simulate grazing dynamics in a different way, then compare the results to infer which type of grazing dynamics are required to match observations. We find that there is dramatic spatial variability in how zooplankton appear to be grazing and that this variability maps well onto the observed phytoplankton concentration, suggesting that the type of zooplankton present may be determined by the amount of prey available.

1 Introduction

Marine net primary production (NPP) accounts for roughly half of global carbon fixation (Falkowski et al., 2000) and supports the biological export of carbon (de la Rocha, 2006) and base of the marine food chain (Armengol et al., 2019). Although oceanographers have historically focused on light (Sverdrup, 1953) and nutrients (Howarth, 1988), increasing experimental (Lima-Mendez et al., 2015; Guidi et al., 2016), observational (Behrenfeld et al., 2013) and modelling (Hashioka et al., 2013; Prowe et al., 2012; Laufkötter et al., 2015; Rohr, n.d.) work has highlighted zooplankton grazing as a critical control on NPP. However, zooplankton grazing dynamics are poorly constrained (Everett et al., 2017), difficult to model (Petrik et al., 2022), and sensitive to environmental change (Richardson, 2008). This uncertainty can lead to large biases in export and secondary production in global marine biogeochemical (BGC) models (Rohr, n.d.).

Empirical laboratory experiments have shown that grazing dynamics (i.e. the manner in which specific grazing rates increase with prey concentration) vary substantially across zooplankton species, age, and size (Hansen et al., 1997; Hirst & Bunker, 2003). However, these studies, which consider the idealized behavior of a single species in a well-mixed environment, are unlikely to be representative of the open ocean. To parameterize relatively coarse global models, oceanographers must understand the mean dynamics of many species, averaged across a patchy ocean, which may diverge dramatically from the dynamics of individual zooplankton (Rohr et al., 2022). Unfortunately, unlike chloro-

phyll and phytoplankton biomass, which can be inferred from ocean optical properties measured remotely (Sathyendranath et al., 2019; Westberry et al., 2008), zooplankton biomass cannot be measured from satellites. Instead, zooplankton must be measured at sea using a variety of different methods (Pakhomov et al., 2020; Pinkerton et al., 2020; Benfield et al., 1998), each with large uncertainties and disparate units (Moriarty et al., 2013), making it difficult to describe the global distribution without large levels of statistical inference (Everett, n.d.; Heneghan et al., 2020).

Without robust global data sets of zooplankton biomass and growth rates, it is difficult, if not impossible, for modellers to prescribe the correct grazing dynamics. This likely contributes to persistent uncertainty in futrue projections NPP (Tagliabue et al., 2021), export production (Fu et al., 2016) and zooplankton biomass (Petrik et al., 2022). Given the increasingly under-constrained nature of heavily parameterized BGC models (Schartau et al., 2017), it is imperative to build out an observationally-informed understanding of the distribution and drivers of grazing dynamics to help constrain them.

Here, were use inverse modelling to reach an initial estimate of the global distribution and drivers of grazing dynamics. In the absence of robust observations of zooplankton biomass, we rely on the well-established influence of grazing dynamics on phytoplankton population dynamics (Gentleman & Neuheimer, 2008; Truscott et al., 1994; Steele, 1974) to asses model skill from the top-down. We run a suite of simulations in a global, coupled ocean-BGC model, parameterized with a wide range of grazing parameters. We determine the optimal parameters required to best match the phenology of the observed phytoplankton seasonal cycle to infer the global distribution of grazing dynamics (**Sec. 3.1**). We then show how this distribution appears to be driven by regional variability in phytoplankton biomass (**Sec. 3.2**) and explain the underlying mechanisms (**Sec. 3.3**). Finally, we address the limitations of these estimates and means to improve them (**Sec. 4.1**), before discussing how they could improve model validation and design (**Sec. 4.2**).

2 Materials and Methods

2.1 The Grazing Formulation in BGC Models

In the simplest BGC models zooplankton grazing occurs between one group of zooplankton on one group of phytoplankton and can be described with a single-prey functional response curve (Gentleman & Neuheimer, 2008). Qualitatively, BGC models are largely split in the type of functional response curve (type II vs III) they use (Rohr et al., 2022). The primary difference between them is that the type II response increases linearly at low prey concentrations, while the type III increases exponentially (**Figure 1**). Either way, this curve, $g([P])$, can be parameterized with a saturation grazing rate (g_{max}; $1/d$), which describes the rate when prey is not limiting, and half saturation concentration ($K_{1/2}$; $mmolC/m^3$), which describes how much prey is required to get there (i.e. $g([K_{1/2}]) = 0.5*g_{max}$). Here we focus on $K_{1/2}$ because it has been shown to have a stronger influence on population dynamics than g_{max} (Rohr et al., 2022).

2.2 Influence of Grazing on Phytoplankton Phenology

Grazing dynamics can influence the shape of seasonal phytoplankton biomass accumulation via the curvature of the functional response, which has either a stabilizing or destabilising influence on phytoplankton population dynamics depending on its concavity (Steele, 1974; Truscott et al., 1994; Gentleman & Neuheimer, 2008). If the functional response is concave upward, then phytoplankton specific loss rates to grazing increase with the size of the population. This creates a negative feedback loop which dampens changes in the size of the phytoplankton population, thereby exerting a stabilizing influence on phenology. Alternatively, downward concavity means phytoplankton spe-

cific loss rates to grazing decline with population growth, creating a destabilizing, positive feedback which amplifies changes in the size of the phytoplankton population.

The shape of the functional response, and thus its stabilizing influence on phenology, is determined by it's response type (II or III) and parameters (particularly $K_{1/2}$). While the parameter values determine the magnitude of curvature and thus the strength of the stabilizing influence, the response type determines the direction. A type II response is always concave downward and thus always destabilizing. However, a type III response has upward concavity below $K_{1/2}$ and thus stabilizing properties a low phytoplankton concentrations. In turn, the grazing formulation has been shown to exert a strong influence on population stability, and thus the size, likelihood, and possibility of phytoplankton blooms, sub-seasonal oscillations, and extinction events (Dunn & Hovel, 2020; Steele, 1974; Adjou et al., 2012; Hernández-García & López, 2004; Truscott et al., 1994; Malchow et al., 2005).

2.3 Model Set up

Ecologically, the true shape of the mean functional response curve in a given swath of the ocean is determined by both the physiological characteristics of individual zooplankton as well as their relative distribution (Rohr et al., 2022). This is difficult to measure in-situ, but can be inferred through inverse modelling via its the top-down influence of grazing dynamics on the simulated phytoplankton seasonal cycle. Here we use a global, coupled ocean-BGC to determine which $K_{1/2}$ values and response types are required to best match the observed phytoplankton seasonal cycle.

The BGC model used, the Whole Ocean Model of Biogeochemistry and Trophic-dynamics (WOMBAT) (Law et al., 2017), is part of the Australian Earth Systems Model (ACCESS-ESM1.5) (Ziehn et al., 2020) and has been used extensively in previous studies (Mortenson et al., 2021; Kwiatkowski et al., 2020; Ziehn et al., 2017; Oke et al., 2013). The ocean model is the global configuration of Modular Ocean Model version 5 (Griffies, 2012). WOMBAT has a relatively simple BGC structure ((Rohr, n.d.)) with 1 phytoplankton and 1 zooplankton group. More complex models include multiple zooplankton grazing on multiple prey types, but we are interested in basin-scale variability in the mean dynamics of the entire plankton community. These can be inferred by tuning single-prey grazing response toward the observed community-averaged phytoplankton phenology as observed from space.

2.4 Model Experiments

We ran a total of 36 global simulations, each with a different grazing formulation. To isolate the influence of grazing, each run was initialized from the same state, embedded in an identical repeat-climatological physical ocean and forced with identical surface flux and freshwater runoff from the Japanese 55-year atmospheric reanalysis surface dataset, JRA55-do (Tsujino et al., 2020). After initialisation, each run was spun up for 5 years to a quasi-steady state, long enough to equilibrate with changes to its grazing formulation. Model output is reported from the fifth year of the simulation and can be considered climatological.

We ran two suites of experiments, using a type III and II functional response. Within each suite we tested 18 different parameters combination: $K_{1/2} = 0.5,\ 1,\ 2,\ 4,\ 8,\ 16$ ($mmolC/m^3$) and $g_{max} = 0.5,\ 1,\ 2\ (1/d)$. These values are consistent with the range that has been derived empirically and used in models historically (Rohr et al., 2022). All other parameters were kept constant and are identical to those in Law et al. (2017).

2.5 Model Skill Assessment

We used two metrics to evaluate the model's ability to recreate the observed phytoplankton seasonal cycle, the correlation coefficient (CC) and coefficient of variation (CV). The CC measures the co-variability between the simulated and observed climatologies, while the CV measures the magnitude of variability relative to the mean (i.e. standard deviation divided by the mean). Together they capture the shape (CC) and strength (CV) of the seasonal cycle. Importantly, both metrics are normalized by (or in the case of CC agnostic to) the mean annual phytoplankton population size to control for the influence of grazing rates on the mean state and isolate its influence on phenology.

For each metric, the seasonal cycle of simulated surface phytoplankton biomass was compared to an 18-year remote sensing climatology (July 2002 - April 2021) from the Carbon-based Productive Model (CbPM) (Westberry et al., 2008). The remote sensing record was interpolated onto the model grid in space (2160x4320 to 300x360) and time (8-day to 5-day resolution) and all time series were centered on the summer solstice. We used observed carbon instead chlorophyll because WOMBAT does not explicitly resolve chlorophyll. However we repeated the entire analysis using the VIIRS chlorophyll record (comparing model carbon to observed chlorophyll) and found qualitatively similar results (**Supplemental Section 1**).

The cost function for model skill was quantified for each run in each grid-cell by subtracting the absolute difference between the modelled (CV_{mod}) and observed (CV_{obs}) coefficient of variation from the correlation coefficient ($CC_{mod,obs}$),

$$\text{Model Skill} = norm(CC_{mod,obs}) - norm(|CV_{mod} - CV_{obs}|) \tag{1}$$

Note, both metrics are normalized across all model output such that their contribution to the cost function is equally weighted and cost function scores can provide a direct comparisons between the skill of runs between the type II and III experiment suites.

For each response type, we consider three sets of 6 runs, with each run using a different $K_{1/2}$ values (0.5,1,2,4,8,16), but a constant g_{max} value across the set. Within each set the cost function score is interpolated between $K_{1/2}$ values using a piece-wise cubic polynomial and the $K_{1/2}$ value with the maximum score is identified (see **Figure 3**). This value is then averaged across all three sets, each of which use a different g_{max} value (0.5,1,2). Finally, very high latitude regions below -55S or above 55N with limited remote sensing coverage were excluded.

3 Results

3.1 Global distribution and drivers of grazing dynamics

The distribution of observed mean annual surface phytoplankton biomass estimated observationally from CbPM (**Figure 1A**) has a striking co-variability with the distribution of grazing dynamics inferred by the optimal $K_{1/2}$ value required to match the observed seasonal cycle (**Figure 1B, C**). We find that more oligotrophic regions with low mean annual phytoplankton biomass require smaller $K_{1/2}$ values to best match the observed phenology (**Figure 1A-C; bluer**), while more eutrophic regions with high mean annual phytoplankton biomass require larger $K_{1/2}$ values (**Figure 1A-C; greener**). Qualitatively, this pattern generally holds regardless of whether a type II (**Figure 1B**) or III (**Figure 1C**) functional response is used to described grazing dynamics or whether remote sensing biomass (**Figure 1A**) or chlorophyll (**Figure S1**) is used to described the observed phenology.

This is remarkably consistent with the community composition which we would expect to inhabit those respective biomes (Everett, n.d.; Heneghan et al., 2020). Ecologically, the value of $K_{1/2}$ at a fixed g_{max} is related to the rate at which zooplankton can capture (rather than consume) prey. Physiologically, the zooplankton which have high prey capture rates are typically rapidly-grazing microzooplankton and filter feeders. However, these zooplankton species are generally unable to consume anything larger than small flagellates, ciliates and cyanobacteria, exactly the sort of phytoplankton that tend to dominate less productive, nutrient-poor, regions such as the gyres. On the other hand slowly-grazing euphausiids, copepods and macrozooplankton tend to have much slower capture rates but are capable of consuming much larger prey, such as dinoflagellates and diatom assemblages, which tend to dominate more productive, nutrient-rich, regions like the coasts and higher latitudes. Our results not only agree that there is substantial diversity in the zooplankton community across the globe but suggest that these distinctions are essential in mechanistically shaping phytoplankton phenology (see **Sec. 3.2**).

Plotting the distribution of mean annual observed surface biomass against the optimal $K_{1/2}$ values required to match its seasonal cycle further clarifies the relationship between bulk phytoplankton biomass and the mean dynamics with which it appears to be grazed (**Figure 1D**). Regardless of functional response type (II - circles; III - diamonds)) or g_{max} value (thin lines), larger $K_{1/2}$ values are required to recreate the seasonal phenology of biomes with more mean annual phytoplankton biomass. Switching from a type III to type II response or increasing g_{max} both increase mean grazing rates and the y-intercept of the regression but have relatively little influence on its slope (**Table S1**; **Figure 1D**). A similar response is seen when using chlorophyll as the predicting variable (**Figure S1D**). Plotting the optimal $K_{1/2}$ value averaged across all three sets of g_{max} values yields our best guess at the relationship between $K_{1/2}$ and mean phytoplankton biomass ([Phyto]).

$$\text{Type II} : K_{1/2} = 15.8[Phyto] - 7.3$$
$$\text{Type III} : K_{1/2} = 15.2[Phyto] - 10.2$$

$$(2)$$

The slope of of this relationship was not particularly sensitive to the selection of g_{max} when a type III response was used (**Supplemental Section 2**. Note that the top and bottom 20% of biomass grid cells are excluded because the relatively coarse ocean model is less suited to resolve end-member biogeochemical scenarios. However, extending the range to biomes considered suggests that the the optimal $K_{1/2}$ value begins to asymptotically approach a minima and maxima in low and high biomass biomes, respectively. This could imply two ecologically distinct biomes rather than a continuum, suggesting a piece wise fit may be more appropriate (**Supplemental Section 3**).

Finally, regardless of g_{max} value or biome, using a type III function response does a consistently better job of recreating seasonal phenology compared to a type II response(**Figure 1D**), scoring 30% better on average (**Table S1**). This is consistent with in-situ (Morozov et al., 2008) and mathematical (Rohr et al., 2022; Morozov, 2010) observations that the downward concavity, prey refuge, and stabilizing properties associated with a type III response may be a better empirical representation of the mean state of a patchy ocean, even if individual zooplankton graze with a type II response (Hansen et al., 1997; Hirst & Bunker, 2003).

3.2 Influence of the grazing formulation on regional bloom phenology

When $K_{1/2}$ is large, phytoplankton phenology tends to exhibit a stronger, well-defined seasonal cycle with less high frequency variability (**Figure 2**; green lines). This is because the grazing formulation does not heavily influence the stability of the system (Gentleman & Neuheimer, 2008; Rohr et al., 2022), allowing bloom phenology to be driven primarily by bottom-up controls, such as light and nutrient availability, which generally follow
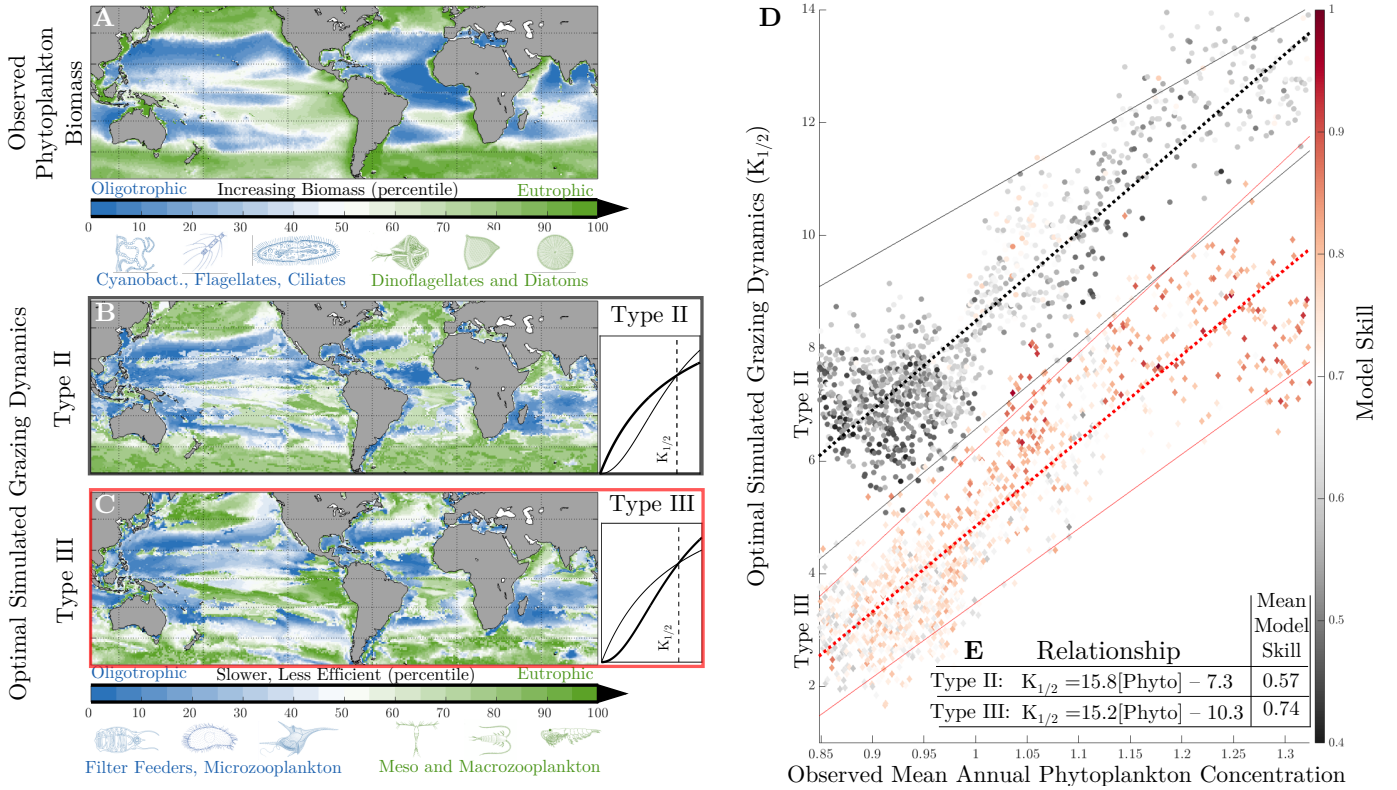
Figure 1. The distribution and drivers of grazing dynamic. **A)** The observed climatological mean annual phytoplankton biomass concentration is plotted as a percentile of the full spatial distribution. Below, the corresponding $K_{1/2}$ parameter required to best recreate the observed phytoplankton seasonal cycle using a **B)** Type II or **B)** III response function is also plotted as a percentile for direct qualitative comparison. Beside each is an example functional response curve for their respective (bolded) response types, both parameterized with the same $K_{1/2}$ and g_{max} values. Below **A)** and **C)** is a schematic of the characteristic phytoplankton associated with low and high biomass waters and the characteristic zooplankton associated with low and high $K_{1/2}$ values. **C)** The optimal $K_{1/2}$ required with a type II (circles; **B)**) and type III (diamonds; **C)**) response are plotted against the corresponding phytoplankton biomass. Points are colored by their mean cost function score, with redder colors indicating increasing model skill. Each point represents then mean of roughly 30 grid cells, binned based on their percentile biomass, with the lowest and highest 20th percentiles excluded. All points and the thick dashed regression were computed by averaging the optimal $K_{1/2}$ value across three experiment suites, each using a different g_{max} values. Uncertainty bounds (thin solid lines) are provided by calculating the relationship using just lowest (0.5) and highest (2) g_{max} values. **E)** The linear regression (dashed lines) and mean model skill is quantified in the inset table and included for all g_{max} values in **Table S1**.
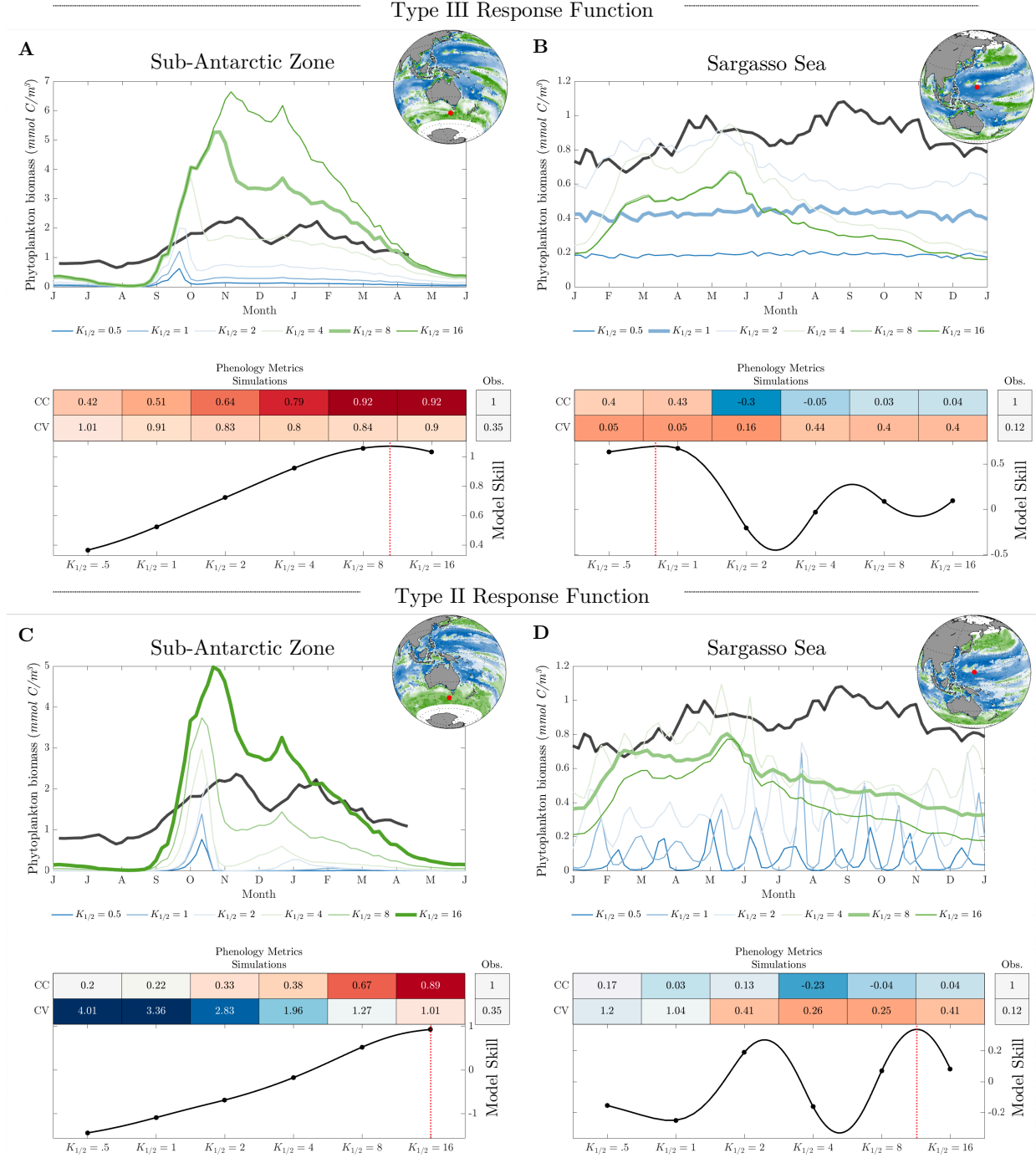
Figure 2. Influence of $K_{1/2}$ and response type on regional phenology. Example seasonal cycles and their model skill are provided from the **A, B** Subantarctic zone south of Australia and **B, D** Sargasso sea. The emergent phenology for all six $K_{1/2}$ values is include for both a **A, B** Type III and **C, D** type II functional response. All simulations use the same identical g_{max} value of $1/d$. **A)** In the upper panel of each subplot the observed (black) and simulated (blue-green) seasonal phytoplankton biomass cycles are plotted with the simulation which best matches the observed phenology boldened. In the lower panel the cost function scoring is demonstrated for each simulation, with the corresponding CC and CV shown above the combine cost function score. Red (blue) color shading indicates better (worse) model skill. The optimal $K_{1/2}$ value is determined by the interpolated maximum of the cost function scores (red line). In the inset map (top right corner) the distribution of optimal $K_{1/2}$ values is shown with the example location marked in red. Note, these distributions are qualitatively identical to Figure 1, with the same percentile-based colorbar, and differs only in that they show results from runs with $g_{max} = 1$ to be consistent with the traces, rather than the mean of all g_{max} values. **B-D** Identical to **A)** but a different location or response function.

a stronger seasonal cycle linked to vertical mixing cycle and the length of the day. In turn, regional phenology is not as sensitive to the whether a type II (**Figure 2A, C**) or III (**Figure 2B, D**) response is used. However, as $K_{1/2}$ decreases, the grazing formulation has a stronger influence on the stability on the system. This influence is stabilizing if a type III response is used but destabilizing if a type II response is used (see **Supplemental Section 4**), resulting in substantively different phenologies depending on the response type used (**Figure 2**; blue tracers). To demonstrate this mechanistic influence of the grazing formulation we consider two cases studies in the sub-Antarctic zone and Sargasso sea, which are generally representative of the seasonal variability in high and low biomass biomes, respectively (see **Figure S4**) .

In the sub-Antarctic zone south of Australia (**Figure 2A, C**) the observed evolution of biomass (black line) exhibits a strong seasonal cycle with an amplitude $\sim 20\%$ greater than its mean and relatively little sub-seasonal variability. It is best recreated using larger $K_{1/2}$ values and exhibits slightly more model skill when a type III response is used. When using a type III response (**Figure 2A**), lower $K_{1/2}$ values reduce the mean biomass but do not systematically modify the CV, leaving the ratio of summer to winter biomass roughly proportional. This occurs because the lower $K_{1/2}$ values systematically increase mean grazing rates, driving biomass down, but increase the first order stability (**Figure S4A**), largely preserving the shape of the seasonal cycle. Alternatively, when using a type II response (**Figure 2C**) response, decreasing $K_{1/2}$ delays bloom initiation but amplifies its acceleration once initiated, leading to smaller, shorter, sharper features and systematically higher CVs. The delayed initiation relative to the type III response occurs because type II response disproportionately increases grazing rates a low biomass concentrations compared to a type III response. The shorter, sharper bloom duration occurs because lowering $K_{1/2}$ in a type II response destabilizes the system (**Figure S4B**), allowing phytoplankton biomass to accumulate exponentially until other stabilizing factors kick in form the bottom-up (i.e. nutrients, self-shading) and rapidly terminate the bloom.

In the Sargasso Sea (**Figure 2B, D**) the observed evolution of biomass (black line) exhibits a much weaker seasonal cycle, with more high frequency variability and an amplitude less than half the size of its mean. It is best recreated using smaller $K_{1/2}$ values and exhibits much more skill when a type III response is used. When using a type III response (**Figure 2A**), highly stable, lower $K_{1/2}$ damp out any seasonality in bottom-up controls and prevent biomass from accumulating. Increasing $K_{1/2}$ systematically increasing the CV by allowing a small seasonal cycle to emerge which is not well correlated with the observed phenology. On the other hand, when using a type II response, while the phenology is nearly identical at high $K_{1/2}$ values, it diverges substantially at low ones. Here, decreasing stability induces unstable predator-prey dynamics which drives higher frequency, sub-seasonal oscillations, leading to higher CVs and poor correlations with the observed phenology.

While the high latitudes and gyres clearly require different $K_{1/2}$ both perform better when a type III response is used. In the sub-Antarctic, a type II grazing leads to blooms that are offset (worse CC) and much sharper (higher CV) than what is observed while in the Sargasso type II grazing can lead to unnatural, sub-seasonal oscillation that are not observed in the remote sensing record. These results further support the use of a type III to represent the complex changes in plankton community composition and its relative distribution, which must be averaged over a coarse model grid cell.

4 Discussion

Of the dominant controls on NPP and subsequent carbon cycling, we have a fairly advanced understanding of the global distribution and drivers of light, temperature, nutrients and deep vertical mixing. However, the distribution and drivers of loss rates, par-

ticularly to grazing, remain largely a blind spot. We have made initial estimates using inverse modelling and discuss their limitations and future directions (**4.1**) in addition to their potential utility to improve BGC and climate models (**4.2**).

4.1 Limitations and future directions

The largest limitation likely stems from the fidelity of the model we have sought to optimize. We have worked to control model bias by repeating experiments in an identical physical ocean. However, if their is a systematic bias somewhere in the simulated seasonal light and nutrient supply, then it is possible that the 'wrong' grazing dynamics could combine with the 'wrong' bottom-up controls to produce the correct phenology, leading us to incorrectly infer that those grazing dynamics were optimal. This could be the case along the equator where there is a disproportionately large model bias in model phytoplankton biomass relative to that of NPP (**Figure S5**), suggesting phytoplankton specific growth rates are too low due to some systematic bias in the bottom-up controls. This may explain why we found slower grazing dynamics (**Figure 1B**; greener) in the equatorial Indian, Atlantic, and Pacific basins than we would have expected from the low mean annual phytoplankton biomass (**Figure 1A**; bluer) observed there. If the model is misrepresenting bottom-up controls as too weak, it make sense that slower than expected grazing is needed to permit biomass accumulation and match the observed phenology. Additional biases may stem from the remote sensing products, which interpolate over cloud cover and cannot capture the complete seasonal cycle at high latitudes, as well as the exact nature of the link between trophic controls and bloom phenology (Behrenfeld et al., 2013; Rohr et al., 2017).Considering these potential biases, it is essential to further refine estimates of the distribution of grazing dynamics with more observationally-focused methods.

4.2 Model Utility

Despite their limitations, our results demonstrate that grazing dynamics vary largely in space and agree qualitatively with our best observational understanding of how zooplankton species are distributed across the ocean (Everett, n.d.; Heneghan et al., 2020). Considering the sensitivity of carbon cycling to grazing (Rohr, n.d.), it is critical for models to build in the mechanisms to both recreate this distribution and allow it to respond to changing physical and environmental drivers. As warming, stratification, and faster wind transform the surface ocean, the ensuing balance of light and nutrients will reshape marine ecosystems, likely favouring different zooplankton species, in different places, with vastly different grazing dynamics. For instance, if increasing stratification dominates increasing wind stress leading to shallower summer mixed layers in the Southern Ocean, then we may expect a shift toward smaller phytoplankton, which have higher light, but lower nutrient, requirements (Pörtner et al., 2019). This shift would be followed by a shift in zooplankton which are better adapted to graze on smaller phytoplankton, such microzooplankton and salpes. Already a southward shift of salpes into regions previous dominated by Euphausiids has been observed (Henschke & Pakhomov, 2019; Steinberg & Landry, 2017). As faster grazers push south the global distribution of net primary, secondary and export production will be substantially altered (Rohr, n.d.). This shift must be captured in BGC models if Earth system and ecosystem models hope to reduce the uncertainty in projections of NPP (Tagliabue et al., 2021), export production (Fu et al., 2016), and fisheries catch (Tittensor et al., 2021) which will be required to accurately predict changes in the oceans capacity to buffer a changing climate and feed a growing population.

4.2.1 Model Validation

Given the large uncertainty in future projections of zooplankton biomass (Petrik et al., 2022) it is clear that the environmental controls on mean grazing dynamics are

not well constrained. There is little convergence in how state-of-the-art BGC represent zooplankton. Although some recent BGC models include 10+ plankton groups (Negrete-García et al., 2022; Sommer et al., 2022; Cael et al., 2021), most CMIP6-class models used in 100+ year ensemble climate projections only include 1-3 zooplankton and phytoplankton groups (Kearney et al., 2021; Rohr, n.d.). It is thus critical to know if competition between these limited functional groups is sufficient to drive an emergent distribution in mean community grazing dynamics that matches reality. Even with the limitations discussed above, we believe that diagnostically computing the apparent mean grazing dynamcis (i.e. fitting a functional response curve to mean grazing rate vs. total prey biomass) and comparing these qualitative distributions to **Figure 1** will help assess model skill and constrain marine carbon cycling in increasingly under-constrained BGC models (Schartau et al., 2017). If the apparent grazing dynamics differ dramatically, or worse, are spatially homogeneous (Law et al., 2017; Zahariev et al., 2008), then it should be clear that other spatially heterogeneous bottom-up controls must be over-tuned to recreate observed heterogeneity in NPP.

4.2.2 Model Development

If explicit competition between limited functional groups is insufficient to resolve the emergent distribution of community averaged grazing dynamics and a sufficiently complex food web is not compatible with the computational cost of high resolution, fully coupled projections (Neelin et al., 2010), then it may be possible to parameterize zooplankton community composition using the relationship inferred in **Figure 1C**. That is, modellers could implicitly represent changes in zooplankton community composition by modifying the $K_{1/2}$ value of a single group as a function of phytoplankton abundance using equation **2** (or those in **Supplemental Section 2)**. This would allow modelers to explicitly modify the mean grazing dynamics, rather than explicitly resolving each of its constitute species, allowing the mean attributes of the zooplankton community to respond dynamically to changing environmental conditions without increasing the number of state variables the model must carry.

Underlying this parameterization are the assumptions that a) bulk phytoplankton biomass follows community composition, with less (more) productive waters inhabited by smaller (larger) phytoplankton (Roy et al., 2013), b) zooplankton community composition is determined by the composition of the prey field (Kiørboe & Hirst, 2014) c) different species of zooplankton graze with systematically different dynamics (Hansen et al., 1997). All three assumptions are generally well supported individually by observations and are together consistent with the emergent relationship between observed phytoplankton biomass and the inferred grazing dynamics required to recreated its phenology (**Figure 1C**). Although there are several key challenges to implementing this relationship (see **Supplemental Section 5**), leveraging it to parameterize functional differences driven by competition could extend well beyond those associated with grazing and allow modellers to vary a collection of biogeochemically important attributes associated with distinctive zooplankton communities at a low computation cost (see **Supplemental Section 5**).

5 Conclusions

These results present a novel, observationally-informed, map of global mean community grazing dynamics, which likely differ dramatically from the behaviour of individual zooplankton species long measured in laboratories. Further refining the observed distribution and drivers of grazing, and how to replicate them in models, will require close collaboration with zooplankton ecologists, but presents an exciting new frontier in chemical oceanography focused on a rigorous understanding of how NPP is controlled from the top-down, a perspective often ignored. Moreover, improving the representation of

zooplankton, which have for too long been treated simply as closure term, could real-
ize dramatic improvements in marine BGC models and our predictions of future ocean
states.

6 Open Research

All model output needed to reproduce the results and associated documentation
can be found at the CSIRO Data Access Portal (https://doi.org/10.25919/wn09-6j31).
The remote sensing products used in Figure 4 can be found at `http://orca.science`
`.oregonstate.edu/2160.by.4320.8day.hdf.carbon2.m.php`. We'd like to thank read-
ers of this document for their attention, and invite them to address any questions to Tyler
Rohr, at tyler.rohr@csiro.au.

Acknowledgments

References

Adjou, M., Bendtsen, J., & Richardson, K. (2012, January). Modeling the influence
from ocean transport, mixing and grazing on phytoplankton diversity. *Ecologi-
cal Modelling*, *225*, 19–27. doi: 10.1016/j.ecolmodel.2011.11.005

Armengol, L., Calbet, A., Franchy, G., Rodríguez-Santos, A., & Hernández-León,
S. (2019, February). Planktonic food web structure and trophic transfer ef-
ficiency along a productivity gradient in the tropical and subtropical Atlantic
Ocean. *Scientific Reports*, *9*(1), 2044. (Publisher: Nature Publishing Group
tex.copyright: 2019 The Author(s)) doi: 10.1038/s41598-019-38507-9

Behrenfeld, M. J., Doney, S. C., Lima, I., Boss, E. S., & Siegel, D. A. (2013).
Annual cycles of ecological disturbance and recovery underlying the
subarctic Atlantic spring plankton bloom. *Global Biogeochemi-
cal Cycles*, *27*(2), 526–540. Retrieved 2022-03-08, from `https://`
`onlinelibrary.wiley.com/doi/abs/10.1002/gbc.20050` (_eprint:
https://onlinelibrary.wiley.com/doi/pdf/10.1002/gbc.20050) doi: 10.1002/
gbc.20050

Benfield, M. C., Wiebe, P. H., Stanton, T. K., Davis, C. S., Gallager, S. M.,
& Greene, C. H. (1998, July). Estimating the spatial distribution of
zooplankton biomass by combining Video Plankton Recorder and single-
frequency acoustic data. *Deep Sea Research Part II: Topical Studies in
Oceanography*, *45*(7), 1175–1199. Retrieved 2022-07-25, from `https://`
`www.sciencedirect.com/science/article/pii/S0967064598000265` doi:
10.1016/S0967-0645(98)00026-5

Cael, B. B., Dutkiewicz, S., & Henson, S. (2021, October). Abrupt shifts in 21st-
century plankton communities. *Science Advances*, *7*(44), eabf8593. Retrieved
2022-12-04, from `https://www.science.org/doi/10.1126/sciadv.abf8593`
(Publisher: American Association for the Advancement of Science) doi:
10.1126/sciadv.abf8593

de la Rocha, C. L. (2006). Chapter 5. The Biological Pump. In *The Oceans and Ma-
rine Geochemistry - 1st Edition* (1st Edition ed.). Pergamon.

Dunn, R. P., & Hovel, K. A. (2020, January). Predator type influences the fre-
quency of functional responses to prey in marine habitats. *Biology Letters*,
16(1), 20190758. (Publisher: Royal Society) doi: 10.1098/rsbl.2019.0758

Everett, J. D. (n.d.). Self-organization of zooplankton communities produces similiar food chain lengths throughout the ocean.

Everett, J. D., Baird, M. E., Buchanan, P., Bulman, C., Davies, C., Downie, R., . . . Richardson, A. J. (2017). Modeling What We Sample and Sampling What We Model: Challenges for Zooplankton Model Assessment. *Frontiers in Marine Science*, *4*, 77. Retrieved 2021-10-19, from `https://www.frontiersin.org/article/10.3389/fmars.2017.00077` doi: 10.3389/fmars.2017.00077

Falkowski, P. G., Scholes, R. J., Boyle, E., Canadell, J., Canfield, D., Elser, J., . . . Steffen, W. (2000, October). The Global Carbon Cycle: A Test of Our Knowledge of Earth as a System. *Science*, *290*(5490), 291–296. doi: 10.1126/science.290.5490.291

Fu, W., Randerson, J. T., & Moore, J. K. (2016, September). Climate change impacts on net primary production (NPP) and export production (EP) regulated by increasing stratification and phytoplankton community structure in the CMIP5 models. *Biogeosciences*, *13*(18), 5151–5170. Retrieved 2022-02-01, from `https://bg.copernicus.org/articles/13/5151/2016/bg-13-5151-2016.html` doi: 10.5194/bg-13-5151-2016

Gentleman, W. C., & Neuheimer, A. B. (2008, November). Functional responses and ecosystem dynamics: How clearance rates explain the influence of satiation, food-limitation and acclimation. *Journal of Plankton Research*, *30*(11), 1215–1231. doi: 10.1093/plankt/fbn078

Griffies, S. M. (2012). *Elements of MOM5, GFDL Ocean Group Technical Report No. 7* (Tech. Rep.). NOAA/Geophysical Fluid Dynamics Laboratory. Retrieved from `https://mom-ocean.github.io/assets/pdfs/MOM5_manual.pdf`

Guidi, L., Chaffron, S., Bittner, L., Eveillard, D., Larhlimi, A., Roux, S., . . . Gorsky, G. (2016, April). Plankton networks driving carbon export in the oligotrophic ocean. *Nature*, *532*(7600), 465–470. (Publisher: Nature Publishing Group tex.copyright: 2016 Nature Publishing Group, a division of Macmillan Publishers Limited. All Rights Reserved.) doi: 10.1038/nature16942

Hansen, P. J., Bjørnsen, P. K., & Hansen, B. W. (1997). Zooplankton grazing and growth: Scaling within the 2-2,-Mm body size range. *Limnology and Oceanography*, *42*(4), 687–704. doi: 10.4319/lo.1997.42.4.0687

Hashioka, T., Vogt, M., Yamanaka, Y., Le Quéré, C., Buitenhuis, E. T., Aita, M. N., . . . Doney, S. C. (2013, November). Phytoplankton competition during the spring bloom in four plankton functional type models. *Biogeosciences*, *10*(11), 6833–6850. (Publisher: Copernicus GmbH) doi: 10.5194/bg-10-6833-2013

Heneghan, R. F., Everett, J. D., Sykes, P., Batten, S. D., Edwards, M., Takahashi, K., . . . Richardson, A. J. (2020, November). A functional size-spectrum model of the global marine ecosystem that resolves zooplankton composition. *Ecological Modelling*, *435*, 109265. Retrieved 2021-08-10, from `https://www.sciencedirect.com/science/article/pii/S0304380020303355` doi: 10.1016/j.ecolmodel.2020.109265

Henschke, N., & Pakhomov, E. A. (2019). Latitudinal variations in Salpa thompsoni reproductive fitness. *Limnology and Oceanography*, *64*(2), 575–584. Retrieved 2022-11-25, from `https://onlinelibrary.wiley.com/doi/abs/10.1002/lno.11061` (_eprint: https://onlinelibrary.wiley.com/doi/pdf/10.1002/lno.11061) doi: 10.1002/lno.11061

Hernández-García, E., & López, C. (2004, September). Sustained plankton blooms under open chaotic flows. *Ecological Complexity*, *1*(3), 253–259. doi: 10.1016/j.ecocom.2004.05.002

Hirst, A. G., & Bunker, A. J. (2003). Growth of marine planktonic copepods: Global rates and patterns in relation to chlorophyll a, temperature, and body weight. *Limnology and Oceanography*, *48*(5), 1988–2010. doi: 10.4319/lo.2003.48.5.1988

Howarth, R. W. (1988, November). Nutrient limitation of net primary production in marine ecosystems. *Annual Review of Ecology and Systematics*, *19*(1), 89–110. (Publisher: Annual Reviews) doi: 10.1146/annurev.es.19.110188.000513

Kearney, K. A., Bograd, S. J., Drenkard, E., Gomez, F. A., Haltuch, M., Hermann, A. J., ... Woodworth-Jefcoats, P. A. (2021). Using Global-Scale Earth System Models for Regional Fisheries Applications. *Frontiers in Marine Science*, *8*, 1121. Retrieved 2021-10-21, from https://www.frontiersin.org/article/10.3389/fmars.2021.622206 doi: 10.3389/fmars.2021.622206

Kiørboe, T., & Hirst, A. G. (2014, April). Shifts in Mass Scaling of Respiration, Feeding, and Growth Rates across Life-Form Transitions in Marine Pelagic Organisms. *The American Naturalist*, *183*(4), E118–E130. Retrieved 2022-11-25, from https://www.journals.uchicago.edu/doi/10.1086/675241 (Publisher: The University of Chicago Press) doi: 10.1086/675241

Kwiatkowski, L., Torres, O., Bopp, L., Aumont, O., Chamberlain, M., Christian, J. R., ... Ziehn, T. (2020, July). Twenty-first century ocean warming, acidification, deoxygenation, and upper-ocean nutrient and primary production decline from CMIP6 model projections. *Biogeosciences*, *17*(13), 3439–3470. Retrieved 2022-03-19, from https://bg.copernicus.org/articles/17/3439/2020/ (Publisher: Copernicus GmbH) doi: 10.5194/bg-17-3439-2020

Laufkötter, C., Vogt, M., Gruber, N., Aita-Noguchi, M., Aumont, O., Bopp, L., ... Völker, C. (2015, December). Drivers and Uncertainties of Future Global Marine Primary Production in Marine Ecosystem Models. *Biogeosciences*, *12*(23), 6955–6984. doi: 10.5194/bg-12-6955-2015

Law, R. M., Ziehn, T., Matear, R. J., Lenton, A., Chamberlain, M. A., Stevens, L. E., ... Vohralik, P. F. (2017, July). The carbon cycle in the Australian Community Climate and Earth System Simulator (ACCESS-ESM1) – Part 1: Model description and pre-industrial simulation. *Geoscientific Model Development*, *10*(7), 2567–2590. doi: 10.5194/gmd-10-2567-2017

Lima-Mendez, G., Faust, K., Henry, N., Decelle, J., Colin, S., Carcillo, F., ... Raes, J. (2015, May). Determinants of community structure in the global plankton interactome. *Science*, *348*(6237). doi: 10.1126/science.1262073

Malchow, H., Hilker, F. M., Sarkar, R. R., & Brauer, K. (2005, November). Spatiotemporal patterns in an excitable plankton system with lysogenic viral infection. *Mathematical and Computer Modelling*, *42*(9), 1035–1048. doi: 10.1016/j.mcm.2004.10.025

Moriarty, R., Buitenhuis, E. T., Le Quéré, C., & Gosselin, M.-P. (2013, July). Distribution of known macrozooplankton abundance and biomass in the global ocean. *Earth System Science Data*, *5*(2), 241–257. doi: 10.5194/essd-5-241-2013

Morozov, A. (2010). Emergence of Holling type III zooplankton functional response: Bringing together field evidence and mathematical modelling. *Journal of Theoretical Biology*, *265*(1), 45–54. doi: 10.1016/j.jtbi.2010.04.016

Morozov, A., Arashkevich, E., Reigstad, M., & Falk-Petersen, S. (2008, October). Influence of spatial heterogeneity on the type of zooplankton functional response: A study based on field observations. *Deep Sea Research Part II: Topical Studies in Oceanography*, *55*(20), 2285–2291. doi: https://doi.org/10.1016/j.dsr2.2008.05.008

Mortenson, E., Lenton, A., Shadwick, E. H., Trull, T. W., Chamberlain, M. A., & Zhang, X. (2021, December). Divergent trajectories of ocean warming and acidification. *Environmental Research Letters*, *16*(12), 124063. Retrieved 2022-03-19, from https://doi.org/10.1088/1748-9326/ac3d57 (Publisher: IOP Publishing) doi: 10.1088/1748-9326/ac3d57

Neelin, J. D., Bracco, A., Luo, H., McWilliams, J. C., & Meyerson, J. E. (2010, December). Considerations for parameter optimization and sensitivity in climate models. *Proceedings of the National Academy of Sciences*, *107*(50), 21349–

21354. Retrieved 2021-10-13, from https://www.pnas.org/content/107/50/21349 (Publisher: National Academy of Sciences Section: Physical Sciences) doi: 10.1073/pnas.1015473107

Negrete-García, G., Luo, J. Y., Long, M. C., Lindsay, K., Levy, M., & Barton, A. D. (2022, December). Plankton energy flows using a global size-structured and trait-based model. *Progress in Oceanography*, *209*, 102898. Retrieved 2022-11-23, from https://www.sciencedirect.com/science/article/pii/S0079661122001574 doi: 10.1016/j.pocean.2022.102898

Oke, P. R., Griffin, D. A., Schiller, A., Matear, R. J., Fiedler, R., Mansbridge, J., ... Ridgway, K. (2013, May). Evaluation of a near-global eddy-resolving ocean model. *Geoscientific Model Development*, *6*, 591–615. doi: 10.5194/gmd-6-591-2013

Pakhomov, E. A., Pshenichnov, L. K., Krot, A., Paramonov, V., Slypko, I., & Zabroda, P. (2020, July). Zooplankton Distribution and Community Structure in the Pacific and Atlantic Sectors of the Southern Ocean during Austral Summer 2017–18: A Pilot Study Conducted from Ukrainian Long-Liners. *Journal of Marine Science and Engineering*, *8*(7), 488. Retrieved 2022-07-25, from https://www.mdpi.com/2077-1312/8/7/488 (Number: 7 Publisher: Multidisciplinary Digital Publishing Institute) doi: 10.3390/jmse8070488

Petrik, C. M., Lou, J., Heneghan, R., Everett, C., Harison, C., & Richardson, A. (2022). Assessment and constraint of mesozooplankton in CMIP6 Earth system models. Global Biogeochemical Cycles. *Preprint https://doi.org/10.1002/essoar.10510705.1*. doi: https://doi.org/10.1002/essoar.10510705.1

Pinkerton, M. H., Décima, M., Kitchener, J. A., Takahashi, K. T., Robinson, K. V., Stewart, R., & Hosie, G. W. (2020, August). Zooplankton in the Southern Ocean from the continuous plankton recorder: Distributions and long-term change. *Deep Sea Research Part I: Oceanographic Research Papers*, *162*, 103303. Retrieved 2022-07-03, from https://www.sciencedirect.com/science/article/pii/S0967063720300911 doi: 10.1016/j.dsr.2020.103303

Prowe, A. E. F., Pahlow, M., Dutkiewicz, S., Follows, M., & Oschlies, A. (2012, August). Top-down control of marine phytoplankton diversity in a global ecosystem model. *Progress in Oceanography*, *101*(1), 1–13. doi: 10.1016/j.pocean.2011.11.016

Pörtner, H., Roberts, D., Masson-Delmotte, V., Zhai, P., Tignor, M., Poloczanska, E., ... Weyer, N. (2019). *IPCC Special Report on the Ocean and Cryosphere in a Changing Climate* (Tech. Rep.). IPCC.

Richardson, A. J. (2008, April). In hot water: zooplankton and climate change. *ICES Journal of Marine Science*, *65*(3), 279–295. Retrieved 2021-10-19, from https://doi.org/10.1093/icesjms/fsn028 doi: 10.1093/icesjms/fsn028

Rohr, T. (n.d.). Marine carbon cycling and sequestration is extremely sensitive to zooplankton grazing in biogeochemical models.

Rohr, T., Long, M., T. Kavanaugh, M., Lindsay, K., & Doney, S. (2017, May). Variability in the Mechanisms Controlling Southern Ocean Phytoplankton Bloom Phenology in an Ocean Model and Satellite Observations. *Global Biogeochemical Cycles*, *31*. doi: 10.1002/2016gb005615

Rohr, T., Richardson, A., Lenton, A., & Shadwick, E. (2022). Recommendations for the Formulation of Grazing in Marine Biogeochemical and Ecosystem Models. *Preprint at https://doi.org/10.1002/essoar.10510767.2*. doi: https://doi.org/10.1002/essoar.10510767.1

Roy, S., Sathyendranath, S., Bouman, H., & Platt, T. (2013, December). The global distribution of phytoplankton size spectrum and size classes from their light-absorption spectra derived from satellite data. *Remote Sensing of Environment*, *139*, 185–197. Retrieved 2022-11-25, from https://www.sciencedirect.com/science/article/pii/S0034425713002629 doi:

10.1016/j.rse.2013.08.004

Sathyendranath, S., Brewin, R. J. W., Brockmann, C., Brotas, V., Calton, B., Chuprin, A., ... Platt, T. (2019, January). An Ocean-Colour Time Series for Use in Climate Studies: The Experience of the Ocean-Colour Climate Change Initiative (OC-CCI). *Sensors*, *19*(19), 4285. doi: 10.3390/s19194285

Schartau, M., Wallhead, P., Hemmings, J., Löptien, U., Kriest, I., Krishna, S., ... Oschlies, A. (2017, March). Reviews and syntheses: Parameter identification in marine planktonic ecosystem modelling. *Biogeosciences*, *14*(6), 1647–1701. doi: 10.5194/bg-14-1647-2017

Sommer, A., Buitenhuis, E., Kiko, R., Fabien, L., Guidi, L., & Le Quéré, C. (2022). *Testing the reconstruction of modelled particulate organic carbon from surface ecosystem components using PlankTOM12 and Machine Learning.* doi: 10.5194/gmd-2022-224

Steele, J. (1974). Stability of plankton ecosystems. In M. B. Usher & M. H. Williamson (Eds.), *Ecological Stability* (pp. 179–191). Boston, MA: Springer US. doi: 10.1007/978-1-4899-6938-5_12

Steinberg, D. K., & Landry, M. R. (2017). Zooplankton and the Ocean Carbon Cycle. *Annual Review of Marine Science*, *9*(1), 413–444. Retrieved 2022-03-07, from https://doi.org/10.1146/annurev-marine-010814-015924 doi: 10.1146/annurev-marine-010814-015924

Sverdrup, H. U. (1953, January). On Conditions for the Vernal Blooming of Phytoplankton. *ICES Journal of Marine Science*, *18*(3), 287–295. doi: 10.1093/icesjms/18.3.287

Tagliabue, A., Kwiatkowski, L., Bopp, L., Butenschön, M., Cheung, W., Lengaigne, M., & Vialard, J. (2021). Persistent Uncertainties in Ocean Net Primary Production Climate Change Projections at Regional Scales Raise Challenges for Assessing Impacts on Ecosystem Services. *Frontiers in Climate*, *3*. Retrieved 2022-02-07, from https://www.frontiersin.org/article/10.3389/fclim.2021.738224

Tittensor, D. P., Novaglio, C., Harrison, C. S., Heneghan, R. F., Barrier, N., Bianchi, D., ... Blanchard, J. L. (2021, October). Next-generation ensemble projections reveal higher climate risks for marine ecosystems. *Nature Climate Change*, 1–9. Retrieved 2021-10-25, from https://www.nature.com/articles/s41558-021-01173-9 doi: 10.1038/s41558-021-01173-9

Truscott, J. E., Brindley, J., Brindley, J., & Gray, P. (1994, June). Equilibria, stability and excitability in a general class of plankton population models. *Philosophical Transactions of the Royal Society of London. Series A: Physical and Engineering Sciences*, *347*(1685), 703–718. (Publisher: Royal Society) doi: 10.1098/rsta.1994.0076

Tsujino, H., Urakawa, S., Nakano, H., Small, R. J., Kim, W. M., Yeager, S. G., ... Yamazaki, D. (2020). input4MIPs.CMIP6.OMIP.MRI.MRI-JRA55-do-1-5-0. Retrieved 2022-03-19, from https://doi.org/10.22033/ESGF/input4MIPs.15017 (Publisher: Earth System Grid Federation Type: dataset) doi: 10.22033/ESGF/input4MIPs.15017

Westberry, T. K., Behrenfeld, M. J., Siegel, D. A., & Boss, E. S. (2008, June). Carbon-Based Primary Productivity Modeling with Vertically Resolved Photoacclimation. *Global Biogeochemical Cycles*, *22*(2). doi: 10.1029/2007GB003078

Zahariev, K., Christian, J. R., & Denman, K. L. (2008, April). Preindustrial, Historical, and Fertilization Simulations Using a Global Ocean Carbon Model with New Parameterizations of Iron Limitation, Calcification, and N 2 Fixation. *Progress in Oceanography*, *77*, 56–82. doi: 10.1016/j.pocean.2008.01.007

Ziehn, T., Chamberlain, M. A., Law, R. M., Lenton, A., Bodman, R. W., Dix, M., ... Srbinovsky, J. (2020, August). The Australian Earth System Model: ACCESS-ESM1.5. *Journal of Southern Hemisphere Earth Systems Science*,

676   *70*(1), 193–214. Retrieved 2021-05-27, from `https://www.publish.csiro.au/`
677   `es/ES19035` doi: 10.1071/ES19035
678   Ziehn, T., Lenton, A., Law, R., Matear, R., & Chamberlain, M.   (2017, July).   The
679   carbon cycle in the Australian Community Climate and Earth System Simu-
680   lator (ACCESS-ESM1) – Part 2: Historical simulations.   *Geoscientific Model*
681   *Development*, *10*, 2591–2614. doi: 10.5194/gmd-10-2591-2017

Supporting Information for "The Global Distribution and Drivers of Grazing Dynamics Estimated from Inverse Modelling"

Tyler Rohr[1,2], Anthony Richardson[3,4], Andrew Lenton[5], Matt Chamberlain[5],

Elizabeth Shadwick[2,5]

[2]Intsitute for Marine and Antarctic Science, University of Tasmania, Hobart, Tasmania, 7000, Australia

[2]Australian Antarctic Partnership Program, Hobart, Tasmania, 7000, Australia

[3]School of Mathematics and Physics, The University of Queensland, St Lucia, Queensland, Australia

[4]Commonwealth Scientific and Industrial Research Organisation (CSIRO) Oceans and Atmosphere, BioSciences Precinct (QBP), St

Lucia, Queensland, 4067, Australia

[5]Commonwealth Scientific and Industrial Research Organisation (CSIRO) Oceans and Atmosphere, Hobart, Tasmania, 7000

Australia

Contents of this file

———

Corresponding author: Tyler Rohr, Australian Antarctic Partnership Program, Hobart, Tasmania, 7000, Australia. (tyler.rohr@utas.edu.au)

December 5, 2022, 5:25am

Text S1. Distribution and drivers of grazing dynamics using the VIIRS chlorophyll record

In **Figure 1** we used phytoplankton carbon biomass estimate remotely from the Carbon-based Productivity Model (Westberry et al., 2008) to compare directly to prognostic phytoplankton biomass resolved in the simulation. However, estimating carbon biomass from space using particle back-scattering involves a different set of assumptions than traditional estimate of phytoplankton abundance which infer chlorophyll concentrations from ocean color. To confirm these differences did not influence our results we repeated the analysis comparing the seasonal cycle of modelled phytoplankton carbon to that of remotely sensed chlorophyll from VIIRS (Sathyendranath et al., 2019). The results were largely consistent (**Figure S1**).

Note, model skill scores appear higher for VIIRS than CbPM (**Table S1**; last column); however, model skill was normalized across all runs using chlorophyll (VIIRS) and all run using carbon (CbPM) independently. Thus, the higher scores for VIIRS do not necessarily mean the modelled seasonal phytoplankton cycle better reflects observed chlorophyll compared to carbon, but rather that the difference between the model skill achieved with the optimal $K_{1/2}$ values compared to sub-optimal $K_{1/2}$ values is larger when comparing to observed chlorophyll.

Text S2. Sensitivity of the relationship between phytoplankton abundance and optimal $K_{1/2}$ value to the functional response type, g_{max} value, and indicator of phytoplankton abundance

The relationship between mean annual phytoplankton abundance and the $K_{1/2}$ parameter required to best recreate its phenology was computed using different functional response types (II, III), g_{max} values (0.5,1,2) and observed indicators for phytoplankton abundance variables (carbon, chlorophyll) and reported in **Table S1**. Across all type III configurations, the relationship was qualitatively consistent. Changing g_{max} in a type III response slightly modified the y-intercept (or mean optimal $K_{1/2}$) but did not substantially influence the slope of the relationship, regardless of if biomass of chlorophyll was being used as the metric for observed phytoplankton abundance. Although, when using a type II response was used, the slope of the relationship was much more sensitive to the value of g_{max}, indicative of its much stronger influence on grazing rates at low prey concentrations and thus population dynamics (Rohr et al., 2022). However, regardless of the g_{max} value used, the type II response consistently exhibited less skill than the type III response when averaged globally across all grid-cells, suggesting it is less suited to represent the mean dynamics in coarse models.

Text S3. Piece-wise linear model Instead of fitting a continuous linear regression to the relationship between phytoplankton abundance and $K_{1/2}$ (**Figure 1D, S1D**) we now consider a piece-wise linear fit. Here we expand the range of biomes included to the 5-90th percentiles, but still exclude very high and low biomass regimes where the model does not perform as well as in the open ocean. Looking at the expanded relationship (**Figure S2**), there are two clear asymptotes when using CbPM biomass as an indicator of phytoplankton abundance but only one when using VIIRS chlorophyll. It is not entirely clear why there is no low asymptote for chlorophyll but it may have to do with

the detection threshold for ocean colour versus backscatter or the fact that at low phytoplankton concentrations the particle back scatter signal may no longer be dominate by phytoplankton.

We then used Bayesian ensemble algorithm for change-point detection and time series decomposition (Zhao et al., 2019) to identify change-points where the relationship began to approach an asymptote. We then fit a piece-wise linear model to the data by assuming a slope of zero across each asymptote beyond the statistically identified change-point and forcing continuity between the asymptotes. These relationships are plotted in **Figure S2**. While they remain qualitatively consistent with the finding that higher $K_{1/2}$ are required drive the phenology of higher biomass biomes, they suggest the transition may occur rather rapidly between two states dominated by slow or rapidly grazing zooplankton.

Collectively, it appears clear that there is an upper and lower bound on realistic $K_{1/2}$ values: roughly 2-10 $mmol/m^3$ when using a type III response (as recommended) or roughly 5-15 when using a tpye II response (not recommended).

Text S4. First order stability of the functional response

The shape of the functional response curve for zooplankton grazing ($g([P])$ influences the shape of phytoplankton phenology primarily via its stabilizing or destabilizing influence on phytoplankton population dynamics (Gentleman & Neuheimer, 2008). The stabilizing influence of grazing is determined by how phytoplankton specific loss rates to grazing (i.e. clearance rates; $Cl = g([P])/[P]$) change in response to changing phytoplankton biomass. If phytoplankton accumulation decreases clearance rates, thereby promoting further population growth, that is a positive feed back with a destabilizing influence.

Alternatively, if phytoplankton accumulation increases clearance rates, thereby damping further population growth, that is a negative feed back with stabilizing influence. The stabilizing influence of the functional response at a given phytoplankton concentration can thereby be quantified is thereby determined by the sign of the first derivation of the clearance rate with respect to the phytoplankton concentration (i.e. $\frac{dCl}{d[P]}$). The value of $\frac{dCl}{d[P]}$ is determined both by the parameters (i.e. $K_{1/2}$) the prescribe the shape of the curve ($g([P])$ as well as the prognostic phytoplankton concentration which is variable in space in time (Rohr et al., 2022).

To capture a mean sense of the stabilizing influence of the functional response across a complete model run and many different phytoplankton concentrations, we define the first order stability as the value of $\frac{dCl}{d[P]}$ at the mean $[P]$ of a given run. The annually-averaged first order stability of our experiments was consistently, necessarily, negative (destabilizing) when a type II response was employed (**Figure S3B**) and positive (stabilizing) when a type III response was employed (**Figure S3A**). In both cases, large $K_{1/2}$ values stretch out the response curve, leading to the depression and linearization of the functional response at low (but common) prey concentrations, slow and steady clearance rates, and very little influence on the stability of the system. Decreasing $K_{1/2}$ in the type II formulations monotonically decreases the first order stability by both directly altering the shape of the functional response curve and indirectly decreasing the prognostic phytoplankton population via increased grazing pressure. Decreasing $K_{1/2}$ in the type III formulations monotonically increases the first order stability of the system. This occurs because increasing Grazing Pressure keeps the annually-averaged phytoplankton

concentration below $K_{1/2}$, where the first order stability increases as $K_{1/2}$ decreases. Note, however, that model configurations with a very low g_{max} or very strong bottom-up growth conditions could buoy phytoplankton populations above $K_{1/2}$, such that decreasing $K_{1/2}$ decreases the first stability of the system, even with a type III response.

Text S5. Challenges and advantages of implementation in a BGC model

First and foremost, the best implementation of this parameterization (**4.3.2**) will require better constraining the relationship between phytoplankton biomass and $K_{1/2}$ in addition to the strength and co-variability of other drivers of zooplankton bio-geogrpahy such as temperature (Brandão et al., 2021) or the relative distribution of prey in models with multiple phytoplankton groups. Using the former may expedite the increase in grazing rates associated with traditional metabolic temperature limitation (Laufkötter et al., 2015) as warmer water also favors more efficient grazing zooplankton species as well (Richardson, 2008). Using the later would largely obviate the assumption that the relative distribution phytoplankton size co-varies with the bulk concentration.

The second major challenge will be determining the space and time scales over which to assume that specific grazing rates should change due to the influence of food scarcity on individual zooplankton versus the influence of zooplankton community composition on mean grazing dynamics. That is, while the value of $K_{1/2}$ determines the instantaneous response of zooplankton grazing rates to food scarcity, it should take longer for $K_{1/2}$ itself to evolve. This is because $K_{1/2}$ reflects the mean physiological characteristics of the entire zooplankton community and can only change at the rate with which community composition can evolve. This timescale likely varies globally and as a function of other

environmental drivers such as temperature (Richardson, 2008). For example, much shorter time periods are needed in communities dominated by asexually-reproducing zooplankton such as salps compared to those dominated by zooplankton with complex, multi-year, life histories, such as euphausiids (Steinberg et al., 2015).

However, getting this right could realize dramatic improvements in BGC models and our predictions of changes to marine carbon cycling. Extending from the assumption that a given optimal $K_{1/2}$ reflects the mean behavior of a particular zooplankton community, other attributes of that community could be additionally parameterized. For instance, crustaceans associated with slower grazing (and larger $K_{1/2}$ values) are typically stronger swimmers. They tend to vertically migrate on daily and seasonal timescales, allowing them to actively transport carbon much faster than microzooplantkon (Steinberg & Landry, 2017). This could be represented by increasing the flux of carbon from zooplankton into the sinking detritus pool (i.e. POC) at low $K_{1/2}$ values, without explicitly including the important role of Diel-vertical migration in carbon transport (see (Archibald et al., 2019)). Other important BGC attributes that vary with zooplankton community composition include the recalcitrance of their detritus and thus the remineralization rates of what they contribute to export production, their sensitivity to temperature, their stoichiometry and carbon content, and their response to seasonal change in the depth of the surface mixed layer.

References

Archibald, K. M., Siegel, D. A., & Doney, S. C. (2019). Modeling the Impact of Zooplankton Diel Vertical Migration on the Carbon Export Flux of the Biologi-

cal Pump. *Global Biogeochemical Cycles*, *33*(2), 181–199. Retrieved 2022-02-03, from `https://onlinelibrary.wiley.com/doi/abs/10.1029/2018GB005983` doi: 10.1029/2018GB005983

Brandão, M. C., Benedetti, F., Martini, S., Soviadan, Y. D., Irisson, J.-O., Romagnan, J.-B., ... Lombard, F. (2021, August). Macroscale patterns of oceanic zooplankton composition and size structure. *Scientific Reports*, *11*(1), 15714. Retrieved 2022-03-07, from `https://www.nature.com/articles/s41598-021-94615-5` doi: 10.1038/s41598-021-94615-5

Gentleman, W. C., & Neuheimer, A. B. (2008, November). Functional responses and ecosystem dynamics: How clearance rates explain the influence of satiation, food-limitation and acclimation. *Journal of Plankton Research*, *30*(11), 1215–1231. doi: 10.1093/plankt/fbn078

Laufkötter, C., Vogt, M., Gruber, N., Aita-Noguchi, M., Aumont, O., Bopp, L., ... Völker, C. (2015, December). Drivers and Uncertainties of Future Global Marine Primary Production in Marine Ecosystem Models. *Biogeosciences*, *12*(23), 6955–6984. doi: 10.5194/bg-12-6955-2015

Richardson, A. J. (2008, April). In hot water: zooplankton and climate change. *ICES Journal of Marine Science*, *65*(3), 279–295. Retrieved 2021-10-19, from `https://doi.org/10.1093/icesjms/fsn028` doi: 10.1093/icesjms/fsn028

Rohr, T., Richardson, A., Lenton, A., & Shadwick, E. (2022). Recommendations for the Formulation of Grazing in Marine Biogeochemical and Ecosystem Models. *Preprint at https://doi.org/10.1002/essoar.10510767.2*. doi: https://doi.org/10.1002/essoar

.10510767.1

Sathyendranath, S., Brewin, R. J. W., Brockmann, C., Brotas, V., Calton, B., Chuprin, A., ... Platt, T. (2019, January). An Ocean-Colour Time Series for Use in Climate Studies: The Experience of the Ocean-Colour Climate Change Initiative (OC-CCI). *Sensors*, *19*(19), 4285. doi: 10.3390/s19194285

Steinberg, D. K., & Landry, M. R. (2017). Zooplankton and the Ocean Carbon Cycle. *Annual Review of Marine Science*, *9*(1), 413–444. Retrieved 2022-03-07, from `https://doi.org/10.1146/annurev-marine-010814-015924` doi: 10.1146/annurev-marine-010814-015924

Steinberg, D. K., Ruck, K. E., Gleiber, M. R., Garzio, L. M., Cope, J. S., Bernard, K. S., ... Ross, R. M. (2015, July). Long-term (1993–2013) changes in macrozooplankton off the Western Antarctic Peninsula. *Deep Sea Research Part I: Oceanographic Research Papers*, *101*, 54–70. Retrieved 2021-11-25, from `https://www.sciencedirect.com/science/article/pii/S0967063715000412` doi: 10.1016/j.dsr.2015.02.009

Westberry, T. K., Behrenfeld, M. J., Siegel, D. A., & Boss, E. S. (2008, June). Carbon-Based Primary Productivity Modeling with Vertically Resolved Photoacclimation. *Global Biogeochemical Cycles*, *22*(2). doi: 10.1029/2007GB003078

Zhao, K., Wulder, M. A., Hu, T., Bright, R., Wu, Q., Qin, H., ... Brown, M. (2019, October). Detecting change-point, trend, and seasonality in satellite time series data to track abrupt changes and nonlinear dynamics: A Bayesian ensemble algorithm. *Remote Sensing of Environment*, *232*, 111181. Retrieved 2022-12-05, from `https://www`
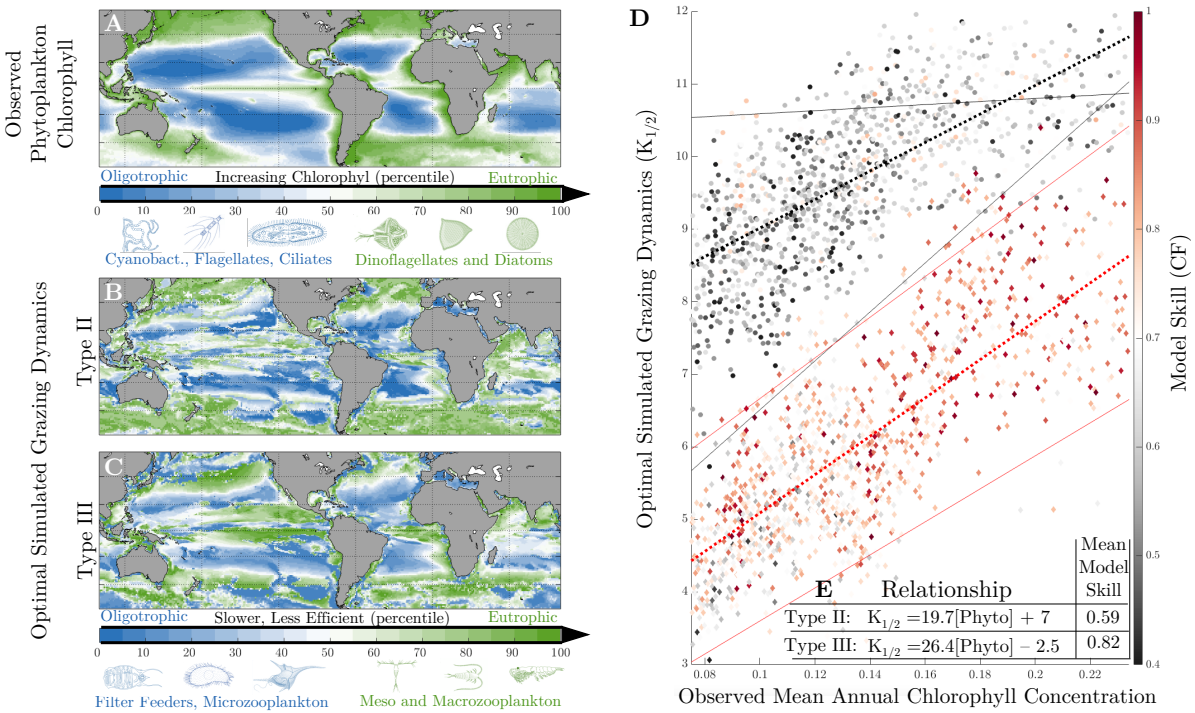
Figure S1. Identical to **Figure 1**, except using VIIRS chlorophyll instead of CbPM carbon biomass to track the observed phytoplankton phenology.

Response Type	g_{max} (d^{-1})	Linear Regression (middle 60 percentile)	Correlation Coefficient	Mean Model Skill
$K_{1/2}$ (mmol C/m³) as a function of Observed Phytoplankton Biomass (CbPM; **Figure 1**)				
Type II	0.5	$K_{1/2} = 15.3[Phyto] - 8.7$	0.74	0.57
Type II	1	$K_{1/2} = 21.7[Phyto] - 13.5$	0.81	0.61
Type II	2	$K_{1/2} = 10.4[Phyto] + 0.2$	0.56	0.56
Type II	Mean	$K_{1/2} = 15.8[Phyto] - 7.3$	0.83	0.57
Type III	0.5	$K_{1/2} = 13.2[Phyto] - 9.7$	0.80	0.75
Type III	1	$K_{1/2} = 15.2[Phyto] - 10.3$	0.74	0.74
Type III	2	$K_{1/2} = 17.2[Phyto] - 10.9$	0.74	0.73
Type III	Mean	$K_{1/2} = 15.2[Phyto] - 10.34$	0.85	0.74
$K_{1/2}$ (mmol/m³) as a function of Observed Phytoplankton Chlorophyl (VIIRS; **Figure S2**)				
Type II	0.5	$K_{1/2} = 33.7[Chl] + 3.1$	0.65	0.65
Type II	1	$K_{1/2} = 23.1[Chl] + 7.6$	0.41	0.64
Type II	2	$K_{1/2} = 2.1[Chl] + 10.4$	0.00	0.47
Type II	Mean	$K_{1/2} = 19.7[Chl] + 7.0$	0.50	0.59
Type III	0.5	$K_{1/2} = 22.7[Chl] + 1.3$	0.51	0.79
Type III	1	$K_{1/2} = 28.5[Chl] + 2.1$	0.56	0.81
Type III	2	$K_{1/2} = 28.5[Chl] + 3.9$	0.48	0.85
Type III	Mean	$K_{1/2} = 26.4[Chl] + 2.5$	0.57	0.82

Table S1.   The relationship between mean annual phytoplankton abundance and the $K_{1/2}$ parameter required to best recreate its phenology. Different relationships refer to different response functions (II,III), g_{max} values (0.5,1,2) and observed phytoplankton variables (Carbon, Chlorophyll). Mean model skill refers to the average cost function score of the optimal $K_{1/2}$ across all grid cells in a given configuration
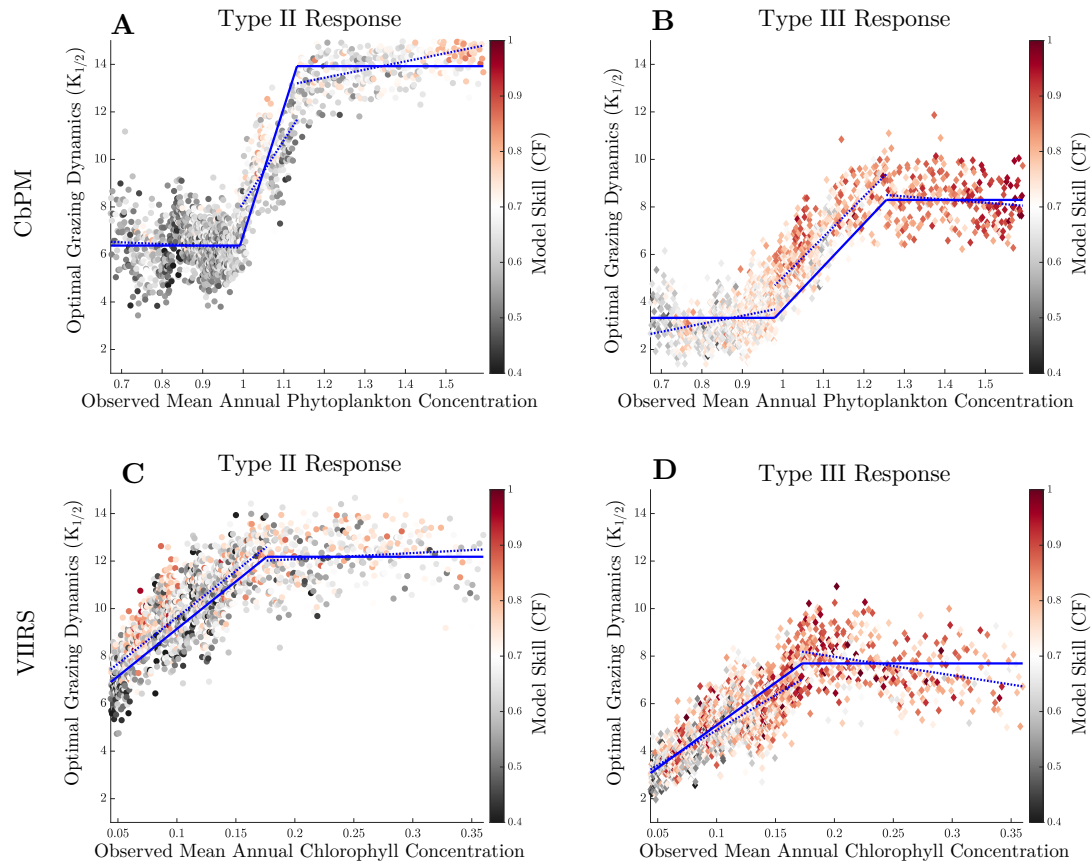
Figure S2.   A piece-wise linear model is fit to the relationship between phytoplankton abundance and the optimal $K_{1/2}$ required to recreate its seasonal cycle when using **A, C)** a type II and **B, D)** a type III response function and **A, B)** CbPM carbon and **C, D)** VIIRS Chlorophyll to represent phytoplankton abundance
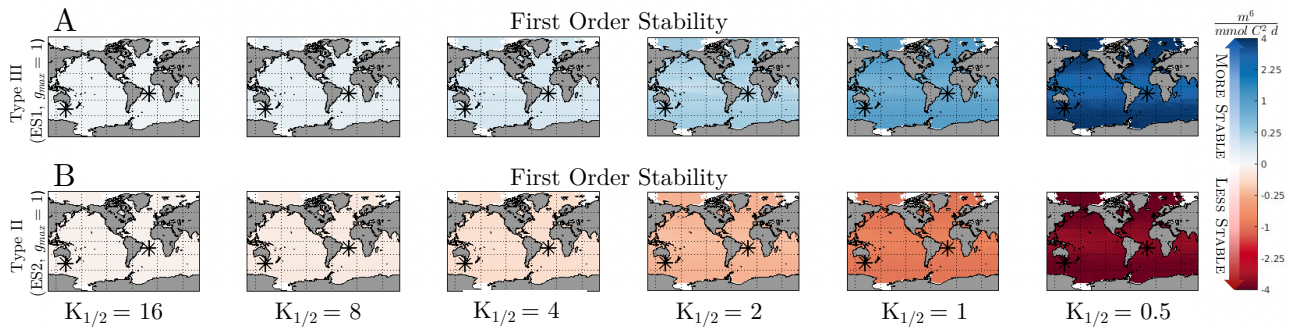
Figure S3.   Sensitivity of ecosystem stability to $K_{1/2}$. Global distributions of the mean-annual first order stability is plotted for all $K_{1/2}$ values, each with a consistent $g_{max} = 1$, and a **A)** type III and **b)** type II functional response.
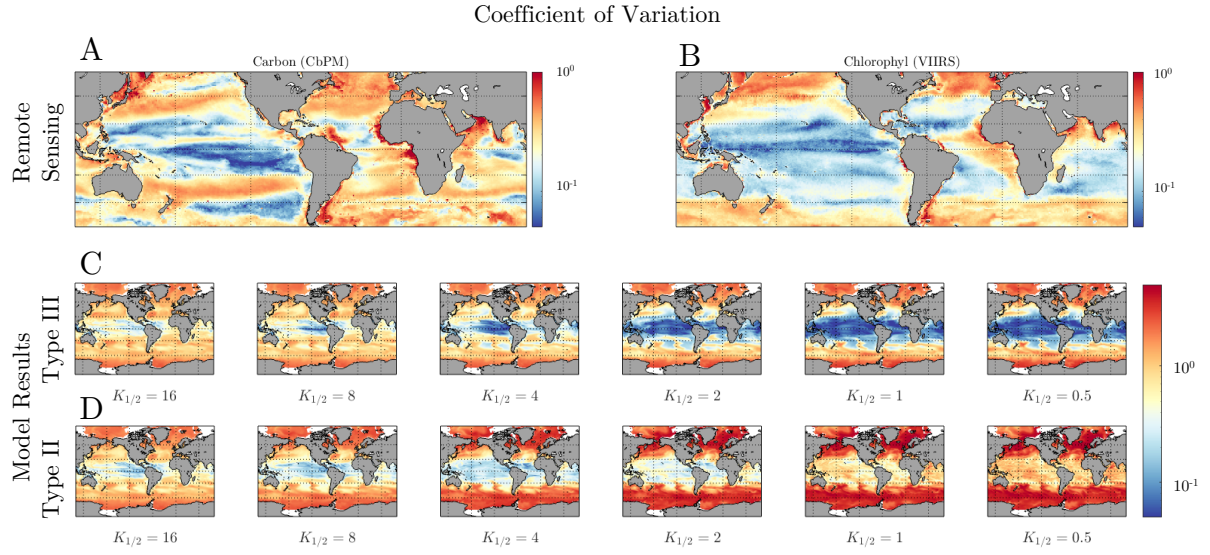
Figure S4. Sensitivity of the strength of the phytoplankton seasonal cycle to $K_{1/2}$.
A, B) The global distribution of observed coefficients of variation, computed from the
seasonal phytoplankton **A)** biomass and **B)** chlorophyll cycles is plotted above the **C, D)**
the distribution of simulated coefficients of variation for all all $K_{1/2}$ values, each with a
consistent $g_{max} = 1$, and a **C)** type III and **D)** type II functional response.
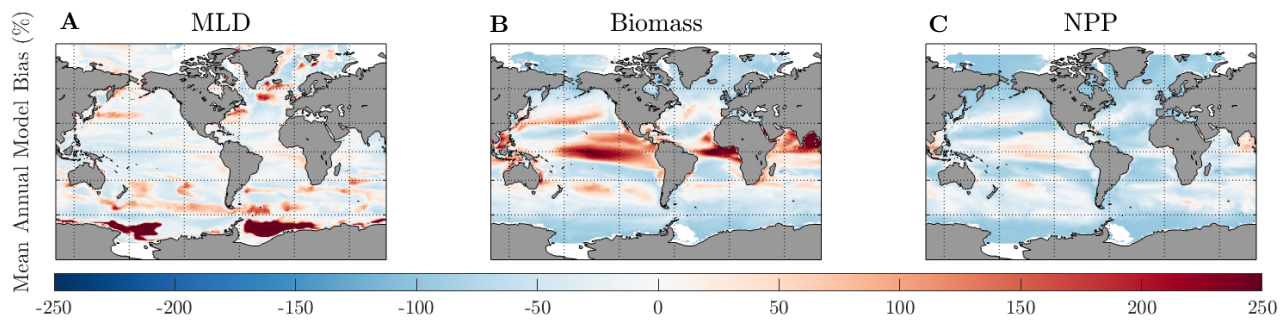
Figure S5. The mean annual model bias is plotted for the **A)** mixed layer depth (MLD) relative to HYCOM reanalysis, **A)** Phytoplankton biomass relative to CbPM and **C)** NPP relative to NPP.